

Curvature effect induce topological phase transitions in two dimensional topological superconductor

Huan-Wen Lai^{a,b}*, Meng-Chien Wang^b, Ching-Ray Chang^{a,b} and Seng-Ghee Tan^c

^a*Quantum information center, Chung Yuan Christian University, Taoyuan, Taiwan.*

^b*Department of Physics, National Taiwan University, Taipei, Taiwan.*

^c*Department of Optoelectric Physics, Chinese Culture University, Taipei, Taiwan.*

{Date: January 23, 2024}

Abstract

Recently, topological superconductor is one of the important topics in condensed matter physics due to the exotic features of quasiparticles resided on the edge, surface and vortex core. In our work, we analyze the two dimensional s+p wave noncentrosymmetric superconductor(NCS) with Rashba spin-orbit coupling in 2D cylindrical coordinate to find the relationship between the topological phase transition and the curvature. With analytical calculation and numerical analyze, we confirm that the topological phase transition in s+p wave NCS in 2D cylindrical coordinate is related to the curvature from band theory perspective.

1 INTRODUCTION

Topological materials indicate a new quantum state of matter in condensed matter physics called topological phase which can't be classified by landau theory and is characterized by the edge or surface state due to a topological character of the bulk wave functions. Besides, from a band theory perspective, the topological phase will not change if we can deform the Hamiltonian from one to the other without closing the gap. The prototypical example to illustrate the topological phase is the integer quantum hall effect [1]. By tuning the magnetic field, the value of hall conductivity is related to an integer number called TKNN invariant [2] which can be calculated by the Berry phase of Bloch state in momentum space that the number of the landau levels are related to the number of edge states. In 2005, Zhang [3] proposed another material called topological insulator, the topological phase transition in this material occurs by band inversion process via strong spin-orbit coupling(SOC) and the gapless edge state is preserved by time-reversal symmetry. Later on, Kane and Mele [4] proposed that the topological insulator is classify to Z_2 invariant which is associated with time reversal symmetry and inversion symmetry. With the theory proposed by Kane and Mele, the concept of symmetry protected topological phase appears and many physicists devote to generalize the relation between the topological phase and discrete symmetries to all spatial dimensions, such as the periodic table proposed by Kitaev [5] and Atland [6] to classify the gapped topological phases of non-interacting fermion, including the strongly correlated systems which can be transform to lattice model by field theory method.

One of the most famous example existing topological phase in strongly correlated systems is topological superconductor [7][8], where the quasiparticles in the edge(surface) state of topological superconductor may exist zero energy Majorana fermions [9], which are the same as their own antiparticles, obeying the Non-Abelian statistics and having the potential of being used as a qubit of fault tolerant topological quantum computing [10][11]. In theory, the superconductors with triplet pairing are the candidate materials where the topological superconducting phase exists, and several theoretical models indicate that the triplet p-wave pairing [11][12] can be induced by strong spin-orbit coupling in hybrid structure [13][14] or certain correlated materials such as non-centrosymmetric superconductors(NCSs) [15][16] which are our main discussion below. The NCSs mixes singlet and triplet pairing due to the lack of inversion symmetry caused by the Rashba spin-orbit coupling. Besides, the phase transition is related to the competing order between the singlet pairing potential and triplet pairing potential. Except for tuning the intrinsic parameters, the topological phase transition can also relate to geometry effect. In previous study, da Costa [17] proposed that the additional terms appear in the Hamiltonian of curve space such as the extra pseudopotential and extra pseudomomentum term in contrast to the flat space case. Based on this result, this idea has been widely used in system with SOC in curve space that the curvature can enhance the value of SOC, affecting the charge and spin transport in nearly free electron system. [18][19] In this paper, we extend this idea to s+p wave NCSs systems to analyze the topological phase transition case. By transforming the Bogoliubov-de Gennes Hamiltonian of NCSs with s+p wave pairing in 2D square lattice into a 2D cylindrical coordinate representing nanotubular form and solving the eigenfunction analytically, we can get the relationship between the curvature and the phase transition point. In section 2, we derive the single band Hamiltonian of two dimensional s+p wave NCSs in square lattice and 2D cylindrical surface. In section 3, we derive the square of eigenenergy of the s+p wave NCSs in 2D cylindrical coordinate. In section 4, we discuss the result between the curvature and phase transition point of the intrinsic parameter and conclude the outcome in section 5.

*Corresponding author
✉ harvey910344@gmail.com

2 MODEL HAMILTONIAN

A. Hamiltonian in square lattice

First, Let's consider the single-band Hamiltonian of s+p wave 2D NCSs in square lattice in terms of the Bogoliubov-de Gennes(BdG) Hamiltonian and Nambu spinor.

$$H(\mathbf{k}) = \sum_{\mathbf{k}} \psi^\dagger H_{BdG} \psi \quad (1)$$

Where H_{BdG} denotes Bogoliubov de Gennes Hamiltonian.

$$H_{BdG} = \begin{pmatrix} \varepsilon - \mu & \alpha(k_y + ik_x) & \Delta_t(-k_y - ik_x) & \Delta \\ \alpha(k_y - ik_x) & \varepsilon - \mu & -\Delta & \Delta_t(k_y - ik_x) \\ \Delta_t(-k_y + ik_x) & -\Delta & -\varepsilon + \mu & \alpha(k_y - ik_x) \\ \Delta & \Delta_t(k_y + ik_x) & \alpha(k_y + ik_x) & -\varepsilon + \mu \end{pmatrix} \quad (2)$$

ψ represents Nambu spinor $(c_{k\uparrow}, c_{k\downarrow}, c_{-k\uparrow}^\dagger, c_{-k\downarrow}^\dagger)^T$, And $\varepsilon, \mu, \alpha, \Delta, \Delta_t$ represent kinetic energy $\frac{\hbar^2 k^2}{2m}$, chemical potential, s-wave pairing potential, p-wave pairing potential respectively. Then diagonalizing the H_{BdG} , we can derive the solution of energy square

$$E_{\pm}^2 = (\varepsilon - \mu)^2 + (\alpha k)^2 + \Delta^2 + \Delta_t k^2 \pm 2\sqrt{k^2[\Delta\Delta_t + \alpha(\varepsilon - \mu)]^2} \quad (3)$$

B. Hamiltonian in cylindrical coordinate

In curve space, the k_x, k_y are no longer the good quantum number. So we need to derive the BdG Hamiltonian from generalized form. The generalized form of BdG Hamiltonian can be written as

$$\begin{pmatrix} \hat{H} & \hat{\Delta} \\ \hat{\Delta}^\dagger & \hat{H}^\dagger \end{pmatrix} \quad (4)$$

Where $\hat{H} = H_{KE} + H_{R-SOC}$ represents the normal state dispersion in 2x2 matrix in terms of kinetic energy and Rashba SOC part. And $\hat{\Delta} = (H_{s-wave} + H_{p-wave})i\sigma_y$ represent s+p wave pairing Hamiltonian in 2x2 matrix.

And based on the previous paper [18], the kinetic term with curvature effect can be written as

$$H_{KE} = -\frac{\hbar^2}{2m} \frac{1}{\sqrt{g}} \frac{\partial}{\partial q^m} \left(\sqrt{g} g^{mn} \frac{\partial}{\partial q^n} \right) - \mu - \frac{\hbar^2}{8m} [(Tr\{\alpha_m^n\})^2 - 4det\{\alpha_m^n\}] \quad (5)$$

The first term is the kinetic energy in generalized coordinate, where the index values are m, n. g is the determinant of the matrix formed by the metric components g^{mn} , m is the effective electron mass in solids. The second term is the pseudopotential induced by curvature effect which relevant to mean curvature and Gaussian curvature of coordinate space, α_m^n are the Weingarten curvature matrix elements for a curved surface.

The Rashba SOC term can be written as

$$H_{R-SOC} = -i\hbar S_{im} \sigma^i g^{mu} \frac{\partial}{\partial q^u} + \frac{1}{2} i\hbar S_{i3} \sigma^i Tr\{\alpha_m^n\} \quad (6)$$

Where σ^i denotes the Pauli matrices, the components of the Rashba tensor are defined as S_{im} .

Next we obtain the pairing potential term, the s wave pairing Hamiltonian is invariant because it is momentum independent. $H_{s-wave} = \Delta i\sigma_y$ And the p-wave pairing Hamiltonian can be representation as

$$H_{p-wave} = \frac{\Delta_t}{\alpha} \left(-i\hbar S_{im} \sigma^i g^{mu} \frac{\partial}{\partial q^u} + \frac{1}{2} i\hbar S_{i3} \sigma^i Tr\{\alpha_m^n\} \right) i\sigma_y \quad (7)$$

Combining each terms metioned above, and transforming coordinate and metric tensor into 2D cylindrical case, the 4x4 BdG Hamiltonian in cylindrical coordinate can be written as

$$\hat{H}_{BdG} = \begin{pmatrix} \hat{P} - u - \frac{1}{8m\rho^2} + \frac{\alpha}{\hbar} p_\varphi & e^{-i\varphi} \frac{i\alpha}{\hbar} p_z & -e^{-i\varphi} \frac{i\Delta_t}{\hbar} p_z & \Delta + \frac{\Delta_t}{\hbar} p_\varphi \\ -e^{-i\varphi} \frac{i\alpha}{\hbar} p_z & \hat{P} - u - \frac{1}{8m\rho^2} - \frac{\alpha}{\hbar} p_\varphi & -\Delta + \frac{\Delta_t}{\hbar} p_\varphi & -e^{-i\varphi} \frac{i\Delta_t}{\hbar} p_z \\ e^{i\varphi} \frac{i\Delta_t}{\hbar} p_z & -\Delta + \frac{\Delta_t}{\hbar} p_\varphi & -\hat{P} + u + \frac{1}{8m\rho^2} + \frac{\alpha}{\hbar} p_\varphi & -e^{i\varphi} \frac{i\alpha}{\hbar} p_z \\ \Delta + \frac{\Delta_t}{\hbar} p_\varphi & e^{-i\varphi} \frac{i\Delta_t}{\hbar} p_z & e^{-i\varphi} \frac{i\alpha}{\hbar} p_z & -\hat{P} + u + \frac{1}{8m\rho^2} - \frac{\alpha}{\hbar} p_\varphi \end{pmatrix} \quad (8)$$

Where $\hat{P} = \frac{\hbar^2 k_z^2}{2m} + \frac{\hbar^2 k_\varphi^2}{2m}$

3 SOLUTION OF THE BOGOLIUBOV-DE GENNES HAMILTONIAN IN CYLINDRICAL COORDINATE

The continuum Bogoliubov-de Gennes Hamiltonian in cylindrical surface can be written as

$$\hat{H}_{BdG} \Psi = E \Psi \quad (9)$$

To solve this equation with corresponding eigenvalue in terms of good quantum number in cylindrical surface, The eigenfunction is written as

$$\Psi = A \begin{pmatrix} e^{i(n-\frac{1}{2})\varphi} \\ e^{i(n+\frac{1}{2})\varphi} \\ e^{i(n+\frac{1}{2})\varphi} \\ e^{i(n-\frac{1}{2})\varphi} \end{pmatrix} e^{i\frac{p}{\hbar}z} \quad (10)$$

Where n is magnetic quantum number with half integer, and A is normalized constant. Combining equation (10) with equation (9), we can get the eigenequation

$$h_{BdG} \Psi = E \Psi \quad (11)$$

The matrix h_{BdG} is equal to

$$h_{BdG} = \begin{pmatrix} h_z + h_1 & i\alpha k_z & -i\Delta_t k_z & \Delta + \frac{\Delta_t}{\rho} \left(n - \frac{1}{2} \right) \\ -i\alpha k_z & h_z + h_2 & -\Delta + \frac{\Delta_t}{\rho} \left(n + \frac{1}{2} \right) & -i\Delta_t k_z \\ i\Delta_t k_z & -\Delta + \frac{\Delta_t}{\rho} \left(n + \frac{1}{2} \right) & -h_z - h_2 & -i\alpha k_z \\ \Delta + \frac{\Delta_t}{\rho} \left(n - \frac{1}{2} \right) & i\Delta_t k_z & i\alpha k_z & -h_z - h_1 \end{pmatrix} \quad (12)$$

Where h_z , h_1 , h_2 denote $\frac{\hbar^2 k_z^2}{2m} - \mu$, $\left(\frac{\hbar^2}{2m\rho^2} \right) (n^2 - n) + \frac{\alpha}{\rho} \left(n - \frac{1}{2} \right)$, $\left(\frac{\hbar^2}{2m\rho^2} \right) (n^2 + n) - \frac{\alpha}{\rho} \left(n + \frac{1}{2} \right)$

respectively.

After diagonalizing h_{BdG} , we can get the energy square which describes electron-like and hole-like energy

$$E^2 = \frac{1}{2} \left[\frac{\hbar^2}{2m\rho^2} (n^2 + n) + \left(\frac{\hbar^2 k_z^2}{2m} - \mu \right) - \frac{\alpha}{\rho} \left(n + \frac{1}{2} \right) \right]^2 + \frac{1}{2} \left[\frac{\hbar^2}{2m\rho^2} (n^2 - n) + \left(\frac{\hbar^2 k_z^2}{2m} - \mu \right) + \frac{\alpha}{\rho} \left(n - \frac{1}{2} \right) \right]^2 + \frac{1}{2} \left\{ \left[-\Delta + \frac{\Delta_t}{\rho} \left(n + \frac{1}{2} \right) \right]^2 + \left[\Delta + \frac{\Delta_t}{\rho} \left(n - \frac{1}{2} \right) \right]^2 \right\} + (\Delta_t^2 + \alpha^2) k_z^2 \pm \frac{1}{2} \sqrt{D} \quad (13)$$

Where D is equal to

$$\begin{aligned} & \left\{ \left[\frac{\hbar^2}{2m\rho^2} (n^2 + n) + \left(\frac{\hbar^2 k_z^2}{2m} - \mu \right) - \frac{\alpha}{\rho} \left(n + \frac{1}{2} \right) \right]^2 - \left[\frac{\hbar^2}{2m\rho^2} (n^2 - n) + \left(\frac{\hbar^2 k_z^2}{2m} - \mu \right) + \frac{\alpha}{\rho} \left(n - \frac{1}{2} \right) \right]^2 + \left[-\Delta + \frac{\Delta_t}{\rho} \left(n + \frac{1}{2} \right) \right]^2 - \left[\Delta + \frac{\Delta_t}{\rho} \left(n - \frac{1}{2} \right) \right]^2 \right\} \\ & + 4k_z^2 \left\{ \alpha \left[\frac{\hbar^2}{2m\rho^2} (n^2 + n) + \left(\frac{\hbar^2 k_z^2}{2m} - \mu \right) - \frac{\alpha}{\rho} \left(n + \frac{1}{2} \right) \right] + \alpha \left[\frac{\hbar^2}{2m\rho^2} (n^2 + n) + \left(\frac{\hbar^2 k_z^2}{2m} - \mu \right) - \frac{\alpha}{\rho} \left(n + \frac{1}{2} \right) \right] + 2\Delta\Delta_t \right\}^2 \\ & + 4k_z^2 \left\{ \Delta_t \left[\frac{\hbar^2}{2m\rho^2} (n^2 + n) + \left(\frac{\hbar^2 k_z^2}{2m} - \mu \right) - \frac{\alpha}{\rho} \left(n + \frac{1}{2} \right) \right] - \Delta_t \left[\frac{\hbar^2}{2m\rho^2} (n^2 - n) + \left(\frac{\hbar^2 k_z^2}{2m} - \mu \right) + \frac{\alpha}{\rho} \left(n - \frac{1}{2} \right) \right] 2\Delta_t \frac{n\alpha}{\rho} \right\}^2 \\ & - 8 \left\{ \left[\frac{\hbar^2}{2m\rho^2} (n^2 + n) + \left(\frac{\hbar^2 k_z^2}{2m} - \mu \right) - \frac{\alpha}{\rho} \left(n + \frac{1}{2} \right) \right] + \left[\frac{\hbar^2}{2m\rho^2} (n^2 - n) + \left(\frac{\hbar^2 k_z^2}{2m} - \mu \right) + \frac{\alpha}{\rho} \left(n - \frac{1}{2} \right) \right] \right\} \alpha \left(\frac{\Delta_t}{\rho} \right) \Delta_t k_z^2 \\ & + 4 \left(\frac{\Delta_t}{\rho} \right)^2 \Delta_t^2 k_z^2 - 16\Delta \left(\frac{\Delta_t}{\rho} \right) \Delta_t^2 k_z^2 \quad (14) \end{aligned}$$

4 RESULT

Based on equation (13), only the first excited state of quasiparticle excitation has possibility to close the gap which is the requirement to cause topological phase transition. We fix the n value to $n = \pm \frac{1}{2}$ and take k_z and p wave pairing potential as the double variable of the energy square E^2 to get the gap closing point in first Brillouin Zone that indicates the critical process of band inversion. With this analysis, there's the relationship between the value of p-wave pairing potential indicating the gap closing point and the value of radius. Then, we compare this result with the square lattice case in section 2 to analyze the comparison between the topological phase transition and curvature effect.

In $n = \pm \frac{1}{2}$, The energy square in equation (13) is equal to

$$E^2 = \frac{1}{2} \left[\frac{5\hbar^4}{32m^2\rho^4} + 2 \left(\frac{\hbar^2 k_z^2}{2m} - \mu \right) + \left(\frac{\alpha}{\rho} \right)^2 + \frac{1}{2} \left(\frac{\hbar^2 k_z^2}{2m} - \mu \right) - \frac{3\hbar^2}{4m\rho^2} \left(\frac{\alpha}{\rho} \right) - 2 \left(\frac{\hbar^2 k_z^2}{2m} - \mu \right) \frac{\alpha}{\rho} \right]$$

$$+ \frac{1}{2} \left[2\Delta^2 - 2\Delta \frac{\Delta_t}{\rho} + \left(\frac{\Delta_t}{\rho} \right)^2 \right] + (\Delta_t^2 + \alpha^2) k_z^2 \pm \frac{1}{2} \sqrt{D_1} \quad (15)$$

$$D_1 = \left[\left(\frac{\hbar^4}{8m^2\rho^4} \right) + \left(\frac{\alpha}{\rho} \right)^2 + \frac{\hbar^2}{m\rho^2} \left(\frac{\hbar^2 k_z^2}{2m} - \mu \right) - \frac{3\hbar^2}{4m\rho^2} \left(\frac{\alpha}{\rho} \right) - 2 \left(\frac{\hbar^2 k_z^2}{2m} - \mu \right) \left(\frac{\alpha}{\rho} \right) - 2\Delta \frac{\Delta_t}{\rho} + \left(\frac{\Delta_t}{\rho} \right)^2 \right]^2$$

$$4k_z^2 \left\{ \alpha \left[\frac{\hbar^2}{4m\rho^2} + 2 \left(\frac{\hbar^2 k_z^2}{2m} - \mu \right) - \frac{\alpha}{\rho} \right] + 2\Delta\Delta_t \right\}^2 + 4k_z^2 \left(\frac{\hbar^2}{2m\rho^2} \right)^2 \Delta_t^2 - 16\Delta \frac{\Delta_t}{\rho} \Delta_t^2 k_z^2 + 4 \left(\frac{\Delta_t}{\rho} \right)^2 \Delta_t^2 k_z^2$$

$$- 8 \left[\frac{\hbar^2}{4m\rho^2} + 2 \left(\frac{\hbar^2 k_z^2}{2m} - \mu \right) - \frac{\alpha}{\rho} \right] \alpha \frac{\Delta_t}{\rho} \Delta_t k_z^2 \quad (16)$$

Based on equation (15), and setting $m = m_0$ (electron mass), $\mu = 0.125\text{eV}$, $a = 5.5 \times 10^{-10}\text{m}$ (lattice constant) for numerical calculations, we can get the result between the radius and the p-wave pairing potential symbolizing the topological phase transition point in different values of s-wave pairing potential and Rashba constant. As shown in Fig.1 and Fig.2. Fig.1 shows the numerical result in $\Delta = 3\text{meV}$ case with three different values of Rashba constant per lattice constant. Trivially, if the radius is very large, the outcome of topological phase transition is nearly the same as the square lattice case. It can be derived by equation (15) where the term depending on the radius ρ can be neglected. In aspect of SOC, with a small Rashba constant per lattice constant, the region of suppression of topological phase transition dominates and the outcome of the region of enhancement of topological transition is similar to the square lattice case. On the other hand, with large Rashba constant per lattice constant, the region of enhancement of topological phase transition dominates and the efficiency of enhancement of topological transition is significant compared to small Rashba constant per lattice constant case. Fig.2 shows the numerical result in $\Delta = 7\text{meV}$ case with three different values of Rashba constant per lattice constant. Likewise, it indicates the similar trends of the topological phase transition as Fig.1 case. However; the fascinating result is that the efficiency of enhancement of topological transition is more conspicuous in $\Delta = 7\text{meV}$ than $\Delta = 3\text{meV}$ case.

5 SUMMARY AND CONCLUSION

In summary, we have shown that the single band s+p wave noncentrosymmetric superconductor in square lattice and 2D cylindrical coordinates. By using analytical considerations, we discover that the topological phase transition depends on the radius relevant to the curvature in 2D cylindrical coordinate. When ρ is very big, the result of topological phase transition in 2D

cylindrical coordinate is nearly the same as the square lattice case. And we notice that in the condition of small s-wave pairing and Rashba constant per lattice constant, the suppression of topological phase transition is dominated in small radius region and the enhancement of the topological phase is not notable in some region of radius. On the other hand, in the condition of big s-wave pairing and Rashba constant per lattice constant, the enhancement of topological phase transition is dominated in small radius region and the enhancement of the topological phase is conspicuous.

- [1] Klitzing, K. V., Dorda, G., & Pepper, M. (1980). New method for high-accuracy determination of the fine-structure constant based on quantized Hall resistance. *Physical review letters*, 45(6), 494.
- [2] Thouless, D. J., Kohmoto, M., Nightingale, M. P., & den Nijs, M. (1982). Quantized Hall conductance in a two-dimensional periodic potential. *Physical review letters*, 49(6), 405.
- [3] Bernevig, B. A., Hughes, T. L., & Zhang, S. C. (2006). Quantum spin Hall effect and topological phase transition in HgTe quantum wells. *science*, 314(5806), 1757-1761.
- [4] Kane, C. L., & Mele, E. J. (2005). Z₂ topological order and the quantum spin Hall effect. *Physical review letters*, 95(14), 146802.
- [5] Kitaev A. (2009). Periodic table for topological insulators and superconductors. In *AIP conference proceedings* (Vol. 1134, No. 1, pp. 22-30). American Institute of Physics.
- [6] Altland, A., & Zirnbauer, M. R. (1997). Nonstandard symmetry classes in mesoscopic normal-superconducting hybrid structures. *Physical Review B*, 55(2), 1142.
- [7] Qi, X. L., Hughes, T. L., Raghu, S., & Zhang, S. C. (2009). Time-reversal-invariant topological superconductors and superfluids in two and three dimensions. *Physical review letters*, 102(18), 187001.
- [8] Qin, W., Gao, J., Cui, P., & Zhang, Z. (2023). two-dimensional superconductors with intrinsic p-wave pairing or nontrivial band topology. *Science China Physics, Mechanics & Astronomy*, 66(6), 267005.
- [9] Yazdani, A., von Oppen, F., Halperin, B. I., & Yacoby, A. (2023). Hunting for Majoranas. *Science*, 380(6651), eade0850.
- [10] Nayak, C., Simon, S. H., Stern, A., Freedman, M., & Sarma, S. D. (2008). Non-Abelian anyons and topological quantum computation. *Reviews of Modern Physics*, 80(3), 1083.
- [11] Ivanov A.D. (2001). Non-Abelian statistics of half-quantum vortices in p-wave superconductors. *Physical review letters*, 86(2), 268.
- [12] Yang, L., Chern, G. W., & Lin, S. Z. (2023). Driven Majorana Modes: A Route to Synthetic $p_x + ip_y$ Superconductivity. *arXiv preprint arXiv:2309.04155*.
- [13] Fu, L., & Kane, C. L. (2008). Superconducting proximity effect and Majorana fermions at the surface of a topological insulator. *Physical review letters*, 100(9), 096407.

- [14] Sau, J. D., Lutchyn, R. M., Tewari, S., & Sarma, S. D. (2010). Generic new platform for topological quantum computation using semiconductor heterostructures. *Physical review letters*, 104(4), 040502.
- [15] Shang, T., Zhao, J. Z., Hu, L. H., Gawryluk, D. J., Zhu, X. Y., Zhang, H., ... & Shiroka, T. (2023). Fully gapped superconductivity and topological aspects of the noncentrosymmetric superconductor TaReSi. *Physical Review B*, 107(22), 224504.
- [16] Lapp, C. J., & Timm, C. (2022). Majorana flat bands at structured surfaces of nodal noncentrosymmetric superconductors. *Physical Review B*, 105(18), 184501.
- [17] da Costa R. (1981). Quantum mechanics of a constrained particle. *Physical Review A*, 23(4), 1982.
- [18] Chang, J.Y., Wu, J. S., & Chang, C. R. (2013). Hamiltonians with Rashba and cubic Dresselhaus spin-orbit couplings on a curved surface. *Physical Review B*, 87(17), 174413.
- [19] Ghee Tan, S., Huang, C. C., Jalil, M., Chang, C. R., & Cheng, S. C. (2019). Resilience of the Spin-Orbit Torque against Geometrical Backscattering. *arXiv e-prints*, arXiv-1908.

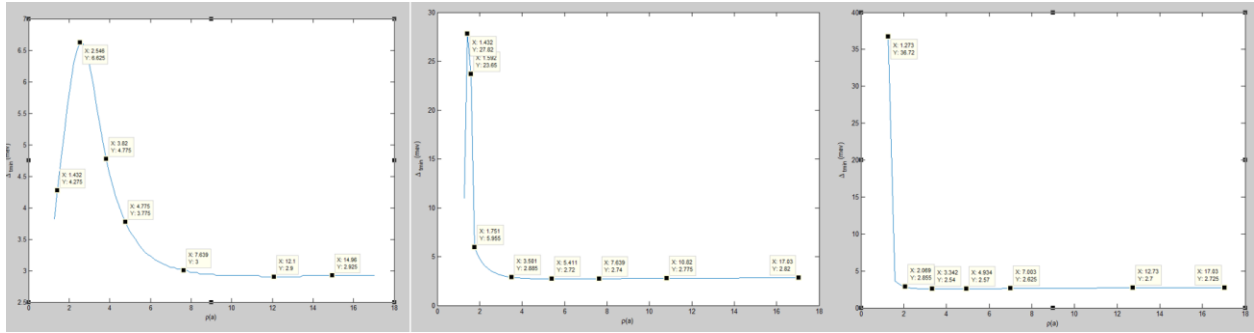


Figure 1: Left: the radius $\rho(a)$ versus Δ_t in $\Delta=3\text{mev}$, $\frac{\alpha}{a}=0$ mev case. Middle: the radius $\rho(a)$ versus Δ_t in $\Delta=3\text{mev}$, $\frac{\alpha}{a}=8.5$ mev case. Right: the radius $\rho(a)$ versus Δ_t in $\Delta=3\text{mev}$, $\frac{\alpha}{a}=17$ mev case.

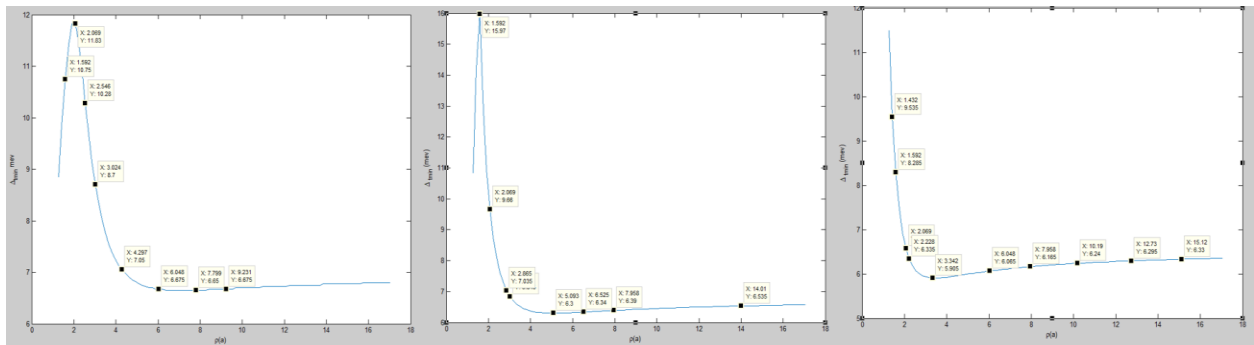


Figure 2: Left: the radius $\rho(a)$ versus Δ_t in $\Delta=7\text{mev}$, $\frac{\alpha}{a}=0$ mev case. Middle: the radius $\rho(a)$ versus Δ_t in $\Delta=7\text{mev}$, $\frac{\alpha}{a}=8.5$ mev case. Right: the radius $\rho(a)$ versus Δ_t in $\Delta=7\text{mev}$, $\frac{\alpha}{a}=17$ mev case.